Austrian Journal of Earth Sciences | Volume 102/2 | 36 - 51 | Vienna | 2009

The Gschliefgraben Landslide (Austria): A Remediation Approach involving Torrent and Avalanche Control, Geology, Geophysics, Geotechnics and Geoinformatics

Robert MARSCHALLINGER[1)*], Christoph EICHKITZ[2)], Harald GRUBER[3)], Kathrin HEIBL[4)], Robert HOFMANN[5)] & Korbinian SCHMID[4)]

[1)] Austrian Academy of Sciences GIScience Research Institute, A-5020 Salzburg; Marschallinger GeoInformatik, A-5201 Seekirchen, Austria;

[2)] Inst. WasserRessourcenManagement, Joanneum Research, A-8010 Graz, Austria;

[3)] Forsttechnischer Dienst, WLV, Sektion Oberösterreich, A-4020 Linz, Austria;

[4)] Moser / Jaritz ZT-Gesellschaft f. Erdwissenschaften / Geologie, A-4810 Gmunden, Austria;

[5)] Hofmann Geotechnik, A-2380 Perchtoldsdorf, Austria;

[*)] Corresponding author, robert.marschallinger@oeaw.ac.at

KEYWORDS

geoinformatics
geotechnics
remediation
landslide
geology

Abstract

The Gschliefgraben (situated lake-side Traunsee, Austria) hosts a big landslide system that has been reactivated only recently, threatening neighbouring buildings and local infrastructure like roads, water-, electricity- and telecommunication conduits. To provide a tracable set of base data for an exhaustive remediation program, thorough geological, geomorphological and geotechnical studies and a detailed monitoring program were accomplished. This article presents some of the most important facts and implications of the above investigations, which were fundamental in stabilizing this huge earth- and debris flow.

The Gschliefgraben, an E-W trending valley, is located at the tectonic border between the Rhenodanubian Flysch and the Ultrahelvetics with predominately marls and sandstones, and the Northern Calcareous Alps with mainly limestones and dolomites. During the Holocene era, this tectonically overprinted mix of competent and incompetent as well as impermeable and highly permeable rocks gave rise to episodic landslide. In the Gschliefgraben area multiple refraction and reflection seismic profiles were measured in several field campaigns lasting over five years. The reflection seismic data were processed using refraction processing after Palmer and the refraction tomography method, with a focus on the suitability of seismic refraction profiles for detecting the basement of landslides. Several horizons were interpreted on these refraction profiles representing changes in velocity but without layer boundaries. These horizons were used to build a three-dimensional model of the subsurface. Surface-related GPS and terrestrial surveying results were combined by geostatistical space-time interpolation, yielding a consistent process model that documents a stepwise cessation of displacements in the light of weather conditions and mitigation measures. Adapted from the above studies, a multiple layer geotechnical model of the soil could be developed which was the basis for defining the mitigation measures that finally lead to stabilizing the landslide motions. Readers are kindly referred to www.oeaw-giscience.org/download/TimeSpace/Gschliefgraben: Geological background information, 2D and 3D graphics and interactive material that cannot be represented adequately in this paper can be downloaded from that site.

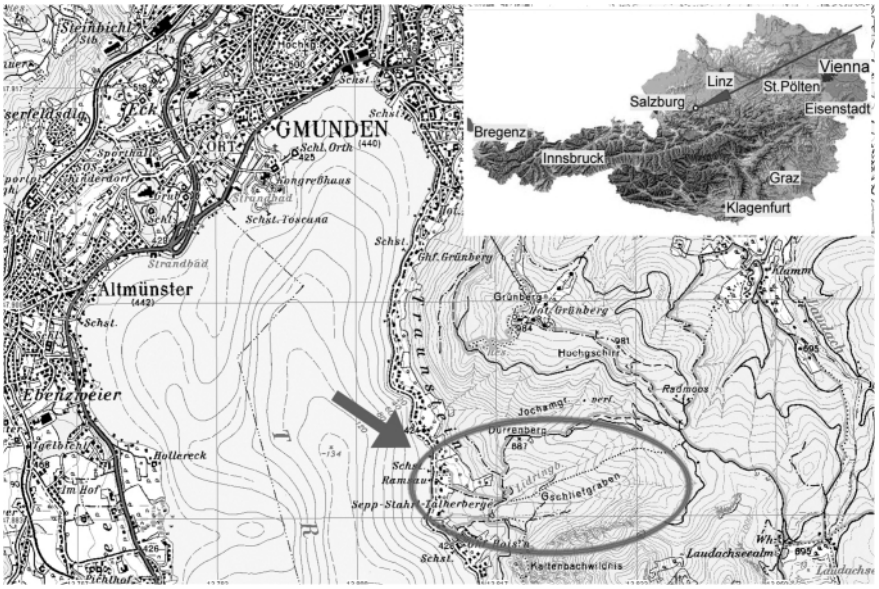

Figure 1: General location of the Gschliefgraben in Austria (www.austrianmap.at). North = top.

Im Gschliefgraben (am Traunsee, Österreich) befindet sich eine große, erst vor kurzer Zeit reaktivierte Hangrutschung. Im Zuge der Sanierung dieses großen Erd- und Schuttstromes wurden umfassende geologische, geomorphologische und geotechnische Studien sowie ein detailliertes Beobachtungsprogramm durchgeführt. Dieser Artikel präsentiert einige der wichtigsten Fakten und Schlussfolgerungen dieser Untersuchungen, welche die Basis für eine Stabilisierung der Gschliefgraben-Rutschung waren.

Der E-W verlaufende Gschliefgraben befindet sich an der Grenze zwischen einerseits Rhenodanubischem Flysch und Ultrahelvetikum, charak-

terisiert durch Mergel und Sandsteine und andererseits den Nördlichen Kalkalpen mit hauptsächlich Kalken und Dolomiten. Die im Gschliefgraben anstehende, tektonisch überprägte Mischung aus kompetenten und inkompetenten bzw. permeablen und impermeablen Gesteinen bedingte während des Holozäns episodische Rutschungsereignisse.

In mehreren Kampagnen wurden Refraktions- und Reflexions Seismikprofile gemessen. Die Interpretation der Auswertungen nach Palmer bzw. der Refraktionstomographiemethode deuten auf mehrere Horizonte mit Geschwindigkeitsunterschieden, jedoch ohne scharfe Grenzen. Die Ergebnisse des Verschiebungsmonitoring Programms - GPS- und terrestrischen Vermessung - wurden mittels geostatistischer Raum-Zeit Interpolation in ein konsistentes Prozessmodell überführt. Aus der Zusammenschau der erwähnten Methoden ergab sich ein geologisch-geotechnisches Mehr-Lagen Modell der Gschliefgrabenrutschung, auf Basis dessen Sanierungsmaßnahmen definiert werden konnten, die eine schrittweise Abnahme der Bewegungen und letztendlich eine Stabilisierung der Gschliefgrabenrutschung ermöglichten. Die Leser werden auf die Internetressource: www.oeaw-giscience.org/download/TimeSpace/Gschliefgraben verwiesen. Geologische Hintergrundinformationen, 2D und 3D Grafiken und interaktives Material können von dort heruntergeladen werden.

1. Introduction and chronicle

The catchment area of the Gschliefgraben drains a huge, geologically caused landslide system, located in Upper Austria (municipality Gmunden), at the east-banks of lake Traunsee.

In late November 2007, presumably triggered by a rock fall in April 2006, an earth flow amounting about 3.8 million m^3 accumulated solids, was set in motion. Dislocation velocity was up to 4.7 m/day at the beginning, and as a result the earth masses threatened to damage 37 estates with 55 buildings and to shift parts of these into the lake, as happened several times during the past centuries (see below). Due to precisely coordinated engineering works, which are described below, this huge debris flow could be stopped. Generally, the Gschliefgraben is a torrent which has a high potential for debris flows with an associated risk exposure for the populated debris fan.

Compiling statements of abutting owners and the city of Gmunden chronicle, Jedlitschka (1974) summarizes the following Gschliefgraben landslide events:

1660: The “Harschengut”, a big farm, is pushed into the lake Traunsee

1734: A big part of the alluvial fan is moved into the lake Traunsee by a debris flow

1884: Rockfall in the “Gamsriese”.

Until 1890: On the ground of the lake Traunsee destroyed farmsteads and fruit trees can be seen.

1891: The ministry of agriculture assigns theTorrent- and Avalanche Control with the investigation of the cause of the landslides.

1910: The Gschliefgraben landslide starts moving. The earth masses shift towards Gschliefort, Eisenau and Kalibauer. A big part of the forest of Ramsau and Eisenau is destroyed. The flat realty of Gschliefort is overlaid with debris in a height of 10 to 15m. The house Gschliefort remains undestroyed.

1910: Inspection of the Gschliefgraben by a commission. A flood wave is suspected by abrupt submerging of the debris fan in the lake Traunsee.

1920: An event occurs in Lidringgraben in direction of Ramsau.

1947: An event occurs in Lidringgraben in direction of Ramsau, the road along the lake Traunsee is covered with mud.

1955: The camping site is accumulated by mud with a depth of 1m.

1987: The camping site is destroyed by a debris flow.

The dimensions of the mass movement were well known to the experts of the torrent and avalanche control, giving rise to a hazard zone map for the Gschliefgraben in 1974. This has been included into the first legally binding land use plan in 1978.

Today, there are 74 objects within the red hazard zone (Fig. 2). The location is well in demand; however, since 1978, there is a construction stop for buildings. Besides endangering the adjoining buildings, the landslide threatens local infrastructure like rural roads, water-, electricity- and communication conduits. Due to the reactivation of the landslide in December 2007, 55 houses had to be evacuated. As a result of the measures taken by the Torrent and Avalanche Control, 40 houses could be reoccupied. By end of August 2008, the evacuation was suspended in consideration of requirements.

Area	3,2 km^2
Height range	422 m to 1691 m (Traunstein)
Length	ca. 3 km
Max. daily precipitation	143, 2 mm (August 12, 1959)
Thunderstorms	25 - 30 days/year
Discharge: HQ150	~32 m^3/s (incl. 15 % sediments)

Table 1: Gschliefgraben catchment area key data.

Figure 2: Hazard zone map, officially approved in 1987. At its periphery, the hazard zone (“red zone”) is wider than 950m.

2. Monitoring

For documentation and planning purposes, a detailed monitoring program has been conducted in the course of the Gschliefgraben landslide remediation project (Tab. 2); some of the monitoring methods are discussed in more detail below.

Monitoring started as early as November 2007. At that time, the registered displacements reached up to 4.7m per day; only very simple displacement monitoring methods were used, like the observation of ranging-poles. These were subsequently complemented and replaced by a state-of-art surveying program.

Remote sensing	Airborne Laserscanning
	Aerial Photographs
	Echo Sounding
Surface - surveying	Survey of drafts
	Observation of ranging-poles
	Monitoring of drafts
	Monitoring of anchors
	Webcam
	Terrestrial survey
	dGPS survey
Depth - surveying	Borehole logs
	Inclinometer
	Well gauges and piezometer
	TDR
	Seismic and geophysics
	Soil mechanics
Hydrology	Precipitation, temperature, barometric pressure
	Discharge in pipes and open channels

Table 2: Monitoring methods applied during the Gschliefgraben landslide remediation.

2.1 Differential GPS

Because of practical difficulties in situating fixed points outside the active land slide area and due to adverse visibilities, a surveying traverse with several stations would have been necessary, bringing about error propagation problems. Therefore, daily dislocations were detected by differential GPS ("dGPS"), providing a positional accuracy of 15-20mm at a measurement time of 30 seconds per point (Energie AG reference network). Since the beginning of dGPS surveying, 153 fixed points were installed, some of which were destroyed by the mitigation measures. In the beginning, measurements were performed on a day-by-day basis, with increasing stabilization of the landslide, measurement intervals could be stepwise expanded. Since May 2009, only a subset of 86 points is surveyed every other week. A total of more than 7500 single measurements is currently available. The results of dGPS surveying are analyzed with a spreadsheet program and plotted in a GIS to be sent to the project team for further interpretation.

2.2 Echo Sounding

A failure of the sub aquatic portion of the debris fan was considered a potential risk. To clarify this risk potential, the sub aquatic debris fan was surveyed by echo sounding campaigns (January, February, May and December 2008). Besides local erosion and a general, minor accumulation at the flanks of the fan, no signs of a large-scale failure could be detected.

2.3 Airborne Laserscanning

For the period of April 2007 to September 2008, five airborne laser scans ("ALS") are available. The precision of the derived digital height models ("DHM", raster cell size 1*1m) is 20cm (horizontal) and 15 cm (vertical). The ALS surveys provide high quality base data for geomorphological and structure-geological mapping as well as for volume-calculations, difference-modeling and deriving profiles or synthetic views used in planning the countermeasures (Fig 4).

ALS based mass balance modeling yielded an erosion of 210000m^3 and an accumulation of 185000m^3, respectively (time period April 2007-September 2008).

3. Geology, hydrogeology and geotechnics (compare related web resources)

The geological and hydrogeological exploration of the Gschliefgraben landslide was carried out by means of various methods. While subsurface explorations were limited chiefly to the area of the current landslide, geological-geomorphologic mapping on a scale of 1:2000 focused in particular on the geology and morphology of the entire Gschliefgraben including its marginal areas. In addition, displacement measurements and observation of the mountain water levels were carried out, which led to the determination of initial emergency procedures (water drainage measures).

3.1 Geology

The central part of the Gschliefgraben consists of rocks of the Ultrahelvetics, which emerge here in the form of a tectonic window below the Rhenodanubian Flysch and the overlying Northern Calcareous Alps. While in the North the Ultrahelvetic borders the Rhenodanubian Flysch throughout, due to tectonics, only the remnants of this unit are preserved in the South. Therefore, the Ultrahelvetic rocks in the South are prevalently in direct contact with the Northern Calcareous Alps, which internally can be divided here into three nappes bottom-up: Kalkalpine Randschuppe, Bajuvarikum and Tirolikum. The tectonic units are cut by a NW-SE striking dextral and a NE-SW striking sinistral fault system, which are characterized by strike-slip faults (Egger et al. 2007).

The Ultrahelvetic stratigraphic succession in the Gschliefgraben is severely torn as a result of the high tectonic stress and the mass movements. Besides coarse-grained sandstones and lime marls of the Lower to Upper Jurassic (Gresten Formation and Blassenstein Formation), there are in particular variegated marls and limy marls of Buntmergelserie as well as, secondarily, glauconitic sandstones and nummulitic limestones, which,

according to Prey (1983), have been deposited from the Lower Cretaceous to the Paleogene.

The Cretaceous sandstones and marls of the Rhenodanubian Flysch that occur along the immediate margin of the Gschliefgraben can be attributed to the Rehbreingraben Formation ("Gaultflytsch"), the Reiselsberg Formation, and the Seisenburg Formation. The Calcareous Alps, which join the central Gschliefgraben in the South, are dominated by limy and dolomitic sedimentary rocks. Within the Kalkalpine Randschuppe appear besides the Upper Triassic Kössen Formation and thick-bedded, dark grey limestones with uncertain stratigraphic position, also siliceous limestones and dark-spotted marl of the Lower Jurassic. Besides a gypsum-clay schist, probably to be classified as Upper Triassic (comp. Prey 1983), Hauptdolomit and Plattenkalk (also Upper Triassic), occurring here in an anticline structure, are prevalent in the Bajuvarikum, which is situated above the Randschuppe.

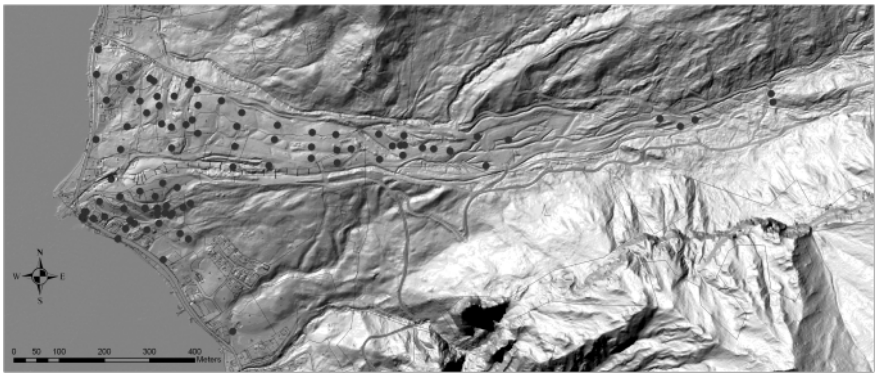

Figure 3: Positions of the current dGPS surveying points. Base map: analytical hillshading, ALS data.

Pleistocene formations are preserved in the form of a thick talus breccia, (outcrops at the so-called Reißeten Schütt) as well as in the form of glacigenous deposits of the Pleistocene Farngruben glacier especially in the upper and southern part of the Gschliefgraben. Since the late Pleistocene, products of weathering and deposits of the various landslide processes were formed, which were very thick particularly in the central Gschliefgraben.

3.2 Hydrogeology

The northern Alpine foreland, which comprises the Gschliefgraben, is characterized by large amounts of precipitation. Especially under barrage weather conditions (moist air from NW-N), high and prolonged precipitation (rain or snow) is apt to occur, therefore the total annual precipitation in the area of the Gschliefgraben is between 1400 and 2000 mm (Jedlitschka 1984).

The catchment area of the Gschliefgraben is mainly determined by morphology. The eastern limit, however, is marked by a subsurface watershed that is located east of the Reißeten Schütt (results of the tracer tests by Baumgartner, 1976). The reason for this are the damming marls (Buntmergel Group) on which the precipitation water is conducted from East, through the lower part of the talus breccia, to West.

Besides the Ultrahelvetic rocks and their products of weathering, the marls of the Kalkalpine Randschuppe as well as the interbeddings of pelites within the Rhenodanubial Flysch act as aquiclude. Accordingly, also the sediments of the mass movements are predominantly impermeable to water. Particularly, the jointed solid rocks in the Gschliefgraben act as joint aquifers. Besides the competent rocks of the Rhenodanubian Flysch and the Ultrahelvetic units, occurring subordinately as far as area is concerned, these are mainly the rocks of the Northern Calcareous Alps. Especially in the Plattenkalk and Hauptdolomit of the Bajuvarikum, water, benefitting from the bedding planes dipping in northern direction, can flow off toward the Gschliefgraben or the talus fans, whereby a strong drainage in western direction (Kaltenbach) must be presumed. Especially the coarse-grained debris could be functioning as a pore aquifer: this means first of all the large talus material as well as the fluvial sediments in the lower parts of the creeks. Further pore aquifers-at least in some areas- are the glacigenous sediments.

Local pore aquifers in coarse-grained sites (eg. rockfall deposits, old land surfaces) can occur in the area of earth/debris flows. Since these aquifers frequently lack free drainage in the lower area, they are partially under pressure.

3.3 Mass Movements

The morphology of the Gschliefgraben area is largely a result of the mass movements that have developed since the melting of the Pleistocene glaciers. Fall, topple, and spread processes dominate in the eastern and southern marginal areas of the Gschliefgraben, which are characterized by hard rocks (Northern Calcareous Alps, Pleistocene talus breccia). On the other hand, slide, flow and creep processes characterize the central part, which is built mainly from Ultrahelvetic marls. These incompetent, soft rocks are especially vulnerable to weathering, because of their intense fragmentation and their comparati-

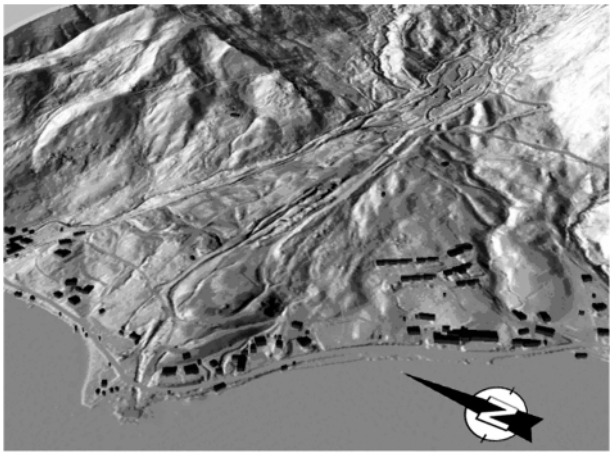

Figure 4: 3D view of the Gschliefgraben landslide (analytical hillshading, ALS, slant view from SW).

vely high content of swellable clay minerals (see 3.4.). In the southern marginal area of the Gschliefgraben there are at the northern foot of the Zirler Schneid the up to 100 m high rock walls of the so-called Ahornwände. They are built mainly from precipitously northward dipping thin- to thick bedded Plattenkalk and Hauptdolomit. Beneath the rock walls there are extended talus fans with blocks of up to 20 m^3 in size. Accordingly, numerous large, relict break-out areas are discernible in the rock walls. The precipitously northward dipping layer surfaces foster the detachment of large rock slabs. A particularly high risk of fall processes exists in the easternmost part of the Ahornwände, in the area of the so-called Gamsriese. In the 18th and 19th century, rockfalls occurred with a volume of, in part, several thousand cubic meters (Weidinger 2005). In the relict crack area, a large rock tower is discernible even today (at least 4,000 m^3). It is only partially connected to the rock wall and its material would probably reach the upper central part of the Gschliefgraben in case of a fall. Moreover, at the foot of the Ahornwände, widespread large cracks and sagged wall parts are discernible as well as signs of relict, but also current topple movements. This is because of the soft, incompetent rocks of the Kalkalpine Randschuppe or gypsum-clay-schist deposits, which deform or are squeezed under the burden of the hard lime and dolomite plates. Similar processes also brought about the formation of tension cracks parallel to the wall, in the area of the so-called Reißeten Schütt in the quaternary talus breccia. As a result, through topple, spread and slide movements, huge, often house-sized blocks got detached from the breccia plate, which were transported further downward in the form of debris flows together with the underlying marls of the Buntmergel. Apart from the numerous tension cracks, a few breccia ridges in danger of falling and toppling as well as current rockfall events southwest of the Reißeten Schütt, this area is currently only slightly active.

Rotational and, subordinated, also translational slides can be found especially in those areas where argillaceous-marly rocks of the Rhenodanubian Flysch or the Ultrahelvetic form the substratum. Besides many smaller ones, larger relict, but also current slides can be found especially at the southern slope of the Gaißbühel, which are situated in weathered marls

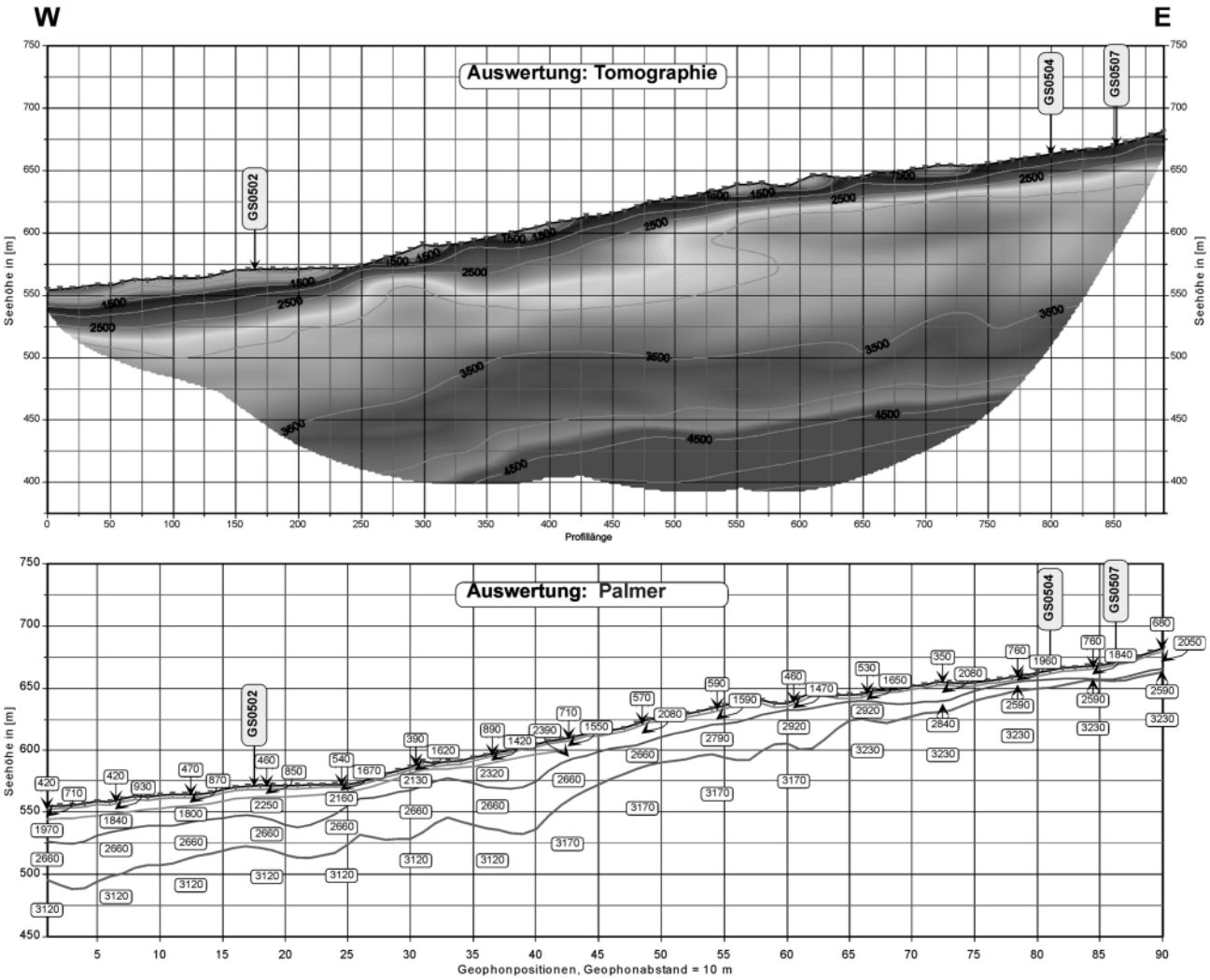

Figure 5: Vertical section showing profile GS0503. The upper picture shows the results using the refraction tomography method. The lower picture shows the results using the classical refraction processing after Palmer (1980). For the Gschliefgraben the refraction tomography method gives better results, because velocity inversion occurs and no abrupt change in velocity with depth can be observed.

and lime marls. Also in the southern part of the Gschliefgraben, time and again landslides have occurred in the Buntmergel Group, overlaid with Calcareous Alpine talus material, as well as in the dark spotted marls of the Kalkalpine Randschuppe, from where—as has been documented e.g., by Weidinger (2007)—partially larger debris flows have emerged that moved into the central part of the Gschliefgraben. The active earth and debris flows, typical of the Gschliefgraben, originate, with the exception of one debris flow, at its middle southern margin, mainly from the central upper part of the area as well as from the upper southern-exposed slopes of the Gaißbühel. Besides the active ones, further, often only vaguely distinctive, earth/debris flows can be identified west of the Reißeten Schütt as well as in the lower part of the Gaißbühel. Their material properties are highly dependent on the respective area of origin.

The earth/debris flows merge in the central, middle part of the Gschliefgraben. From there, the deposited material is transported by fluvial conveyance or—as in 2007— in the form of a large debris flow toward (lake) Traunsee. The deposits of these large mass movements make up the debris cone, approximately 1 km in width, which has been forming below the Gschliefgraben ever since the melting of the glacial glaciers. Baumgartner et al. (1982) divided the debris cone in four earth/debris flow systems of different age. From old to young, these are the systems “Hoisn”, “Ramsau”, “Kalibauer” and the earth/ debris flow event of 1910. The debris fan is characterized by typical flow structures such as bulges, banks, humps, and hollows, which, however, depending on their age, display more or less overprinting as a result of erosion processes. At the end of the debris flow deposits, more or less strongly developed transverse ridges have formed. The most conspicuous component of the earth/debris flows are giant, at times up to 100 m^3 blocks. They consist mainly of the quaternary talus breccia of the Reißeten Schütt and of dark lime materials, which probably are predominantly Plattenkalk from the Ahornwände area. To a large degree, the deposits of the current debris flow of 2007/2008 have in the meantime been anthropogenically overprinted as a result of the mitigation and safety measures.

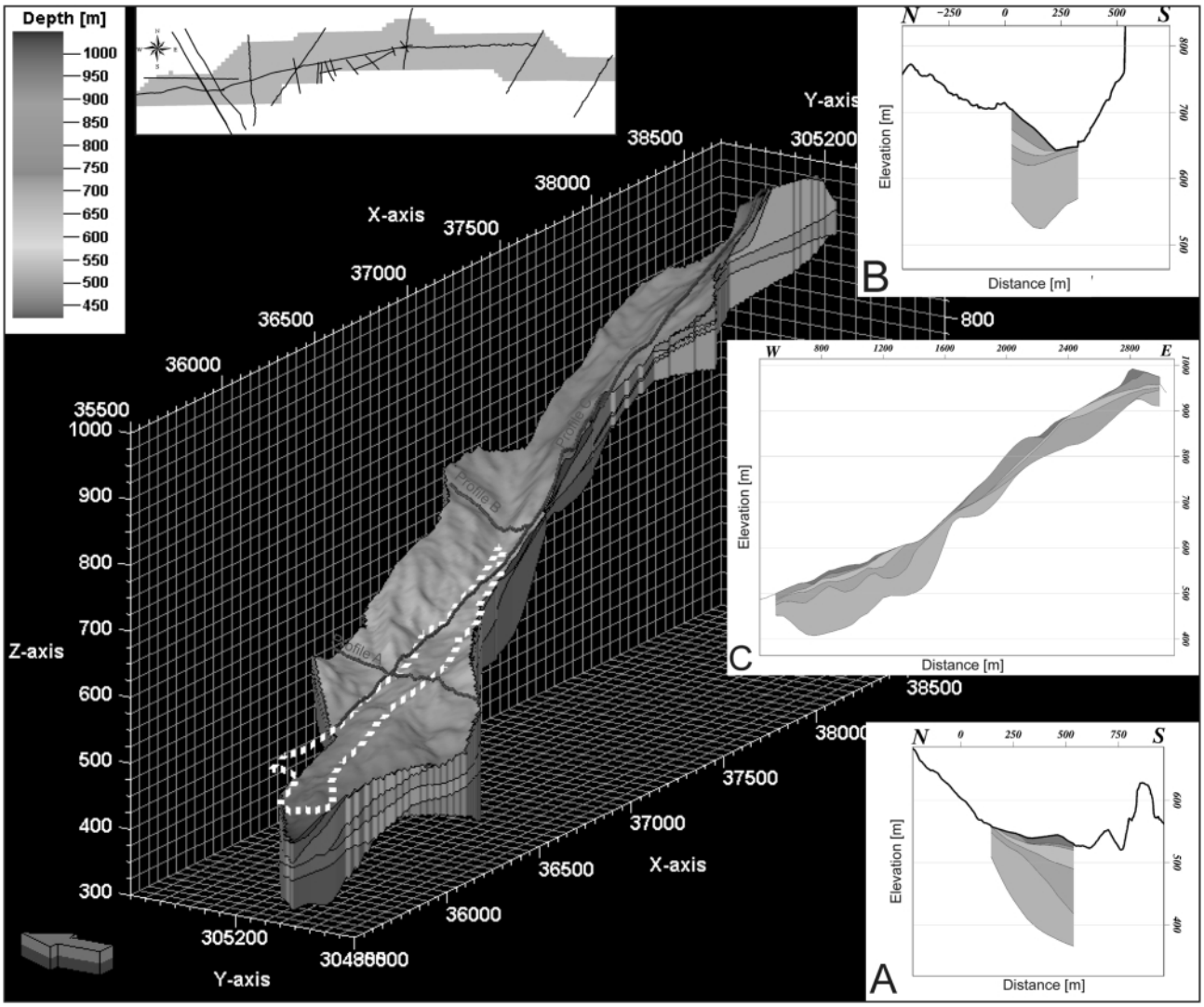

Figure 6: Final model derived from seismic refraction data. The upper left legend shows the elevation of the surface. Next to the legend is a small map showing the position of the seismic refraction profiles (black) and the shape of the model (blue). On the right are three vertical profiles, their position is indicated with the red lines on top of the model (profiles A-C). The dotted white line shows the surface extension of the last land slide.

3.4 Subsurface Exploration

Since the onset of the landslide, a subsurface exploration program by means of core borings has been initiated and constantly expanded. Eleven of the thirteen bores are spread along the foot area of current as well as ancient landslide events to gain insights into the substratum, and the dimension of the landslide and further, to set up measuring points for inclinometer and water pressure. Two core bores were sunk into the slightly more elevated zone of depletion of the landslide to gain insights into their substratum and to establish measuring points for ground displacement measurements in this location.

Boring and test pits (only in the upper Gschliefgraben area) showed, that the thickness of the landslide deposits ranges between 10 meters in the middle Gschliefgraben and more than 170 m at the lake level of Traunsee. Drillings established the sheeting of the earth/debris flow cone of the Gschliefgraben. A large part of the explored soils is represented by sediments of several earthflow events which were deposited since the late Pleistocene (Baumgartner & Sordian 1982). These deposits are built up by some silty argillaceous matrix, which contains various portions of coarse components. A good quarter of the matrix is composed of swellable clay minerals (findings of the Geological Survey of Austria, Vienna). According to ÖNORM B 4400 it could be classified as “ausgeprägt bis mittelplastischer Ton /Schluff”. The included components range from sizes of a sand grain to blocks with a size of several cubic meters. Dark and bright Calcareous Alpine limestone is predominant among the pebble and stone components, while the larger blocks almost exclusively consist of talus breccia. Mudflow deposits could be also discerned which were marked by a high content of slightly rounded, coarse components. Because of their coarse grain content, mudflow deposits are mostly water-bearing. Mountain water is under pressure due to the lateral uphill spreading of these sediments. These ground layers, which are dominated by coarse grains, could partially as well be characterized as old surfaces, where weathering caused the flushing out of fine matter and led to an accumulation of coarse components. The same mountain water situation as in the mud flow deposits can be expected here. Frequently, the layers of repeated debris and mud flows are mixed by later movements.

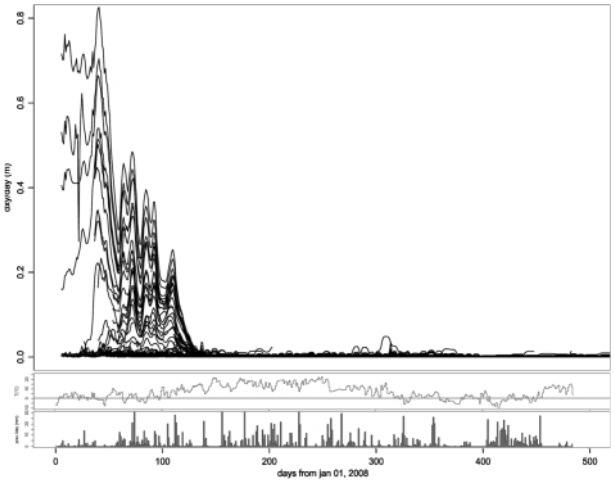

Figure 7: Time series graphs of Gschliefgraben displacement and weather monitoring data. Abscissa: time (days, range=01 Jan. 2008 till 31 May 2009). Ordinates: top – displacements (dxy, m/day) as from surveying (first differences, from interpolated time series), middle - temperature, bottom - precipitation. See text for details.

3.5 Measurements

According to depth and findings of the exploration (e.g., ground water bearings on various levels) inclinometer tubes, piezometers, and water gauges were attached to the exploration drillings.

Out of a total of ten inclination measuring points, movements/deformations were noticed in five points. Two of them were soon destroyed because of strong deformation and could provide movement information only between December 2007 and mid-January 2008. From the remaining measuring points, it is known, that movements in the foot area were clearly noticed until mid-May/mid-June 2008. Surfaces of rupture were established on average between 16 and 19 m under the top ground surface. On the northern front, total displacements of about 5 cm were measured. For the southern foot area of the slope movement, turned form the western, to a southwestern direction a total displacement of 3 cm was observed. Besides the inclinometer measurements, TDR was implemented (Singer et al. 2008). With reference to inclinometer measurements, generally lesser movements were established in TDR measurements because coaxial cable installation was connected to an inclinometer tube in the borehole. Generally, here too, movements could be established until May/June in the foot area since their discovery in December 2007 and their decrease beginning in March 2008. Phases of the main movement, which could be recorded by control methods, occurred in January and February.

In comparison to inclinometer, the TDR measurements generally show a significantly reduced (by an installation with the inclinometer tube caused) amount of movement and the movements become visible in the coaxial cable very late. By contrast, this continuous measurement using a data logger provides a very good insight of the time-dependent movement of the slope and detailed information on speed development in a quality, which could not be provided by individual inclinometer measurements. In addition, TDR is more durable. Unlike the inclinometer, using TDR, the movement direction cannot be established and it can’t afford the precision.

3.6 Wells as Emergency Measures

Based on displacement measurements which showed that most of the sliding surfaces are located between 16 m and 19 m below the top ground surface and are frequently accompanied by water-saturated layers that are under hydrostatic pressure, it was decided to use the sinking of simple gravity bore wells for draining the water saturated layers, with each of them being about 20 meters deep. To lower the pressure head in the water-bearing layers to a larger extent, a gallery-like layout was chosen. By draining, the wells brought about an increased shear resistance in the surrounding ground. This effect could be clearly seen from shearing surfaces, which appea-

red up to the surface before the gallery of wells. It is planned to create a drainage system for the wells, which provides a free downhill flow of the water along the slope.

3.7 Slope Movement Observations in the Foot Area

Parallel to displacement measurements, visual inspections of the foot area of recent slope movements were performed, during which new morphological forms were documented. In the northern foot area, at the end of January 2008, surface movements were limited for a longer period of time to the frontal area, at the height of 468 above sea level. In the end of February 2008, a major deformation by compression was established, which was soon followed by other such deformations. Besides deformations by compression, shear cracks were formed due to differential movements towards the West. Finally superficial movements were visible up to a height of 452 m above sea level. In the southern foot area, south of the Gschliefbach trough up to the stable ancient landslide masses, indications of movements could be discerned in the form of compression bulges and shear cracks, until down to the Traunsteinstraße in the end of January. Until the end of February, progressing movements, increases, and new formations of shear cracks occurred, mostly in southwestern direction. Since the beginning of January, intensive bulges were formed in the steep, formerly wooded slope in the southwestern part of the moved foot area. After the strongest periods of movements recorded in January, the area has been over-printed through the removal of soil material. Already known shear cracks kept reappearing even after the slopes had been dug away.

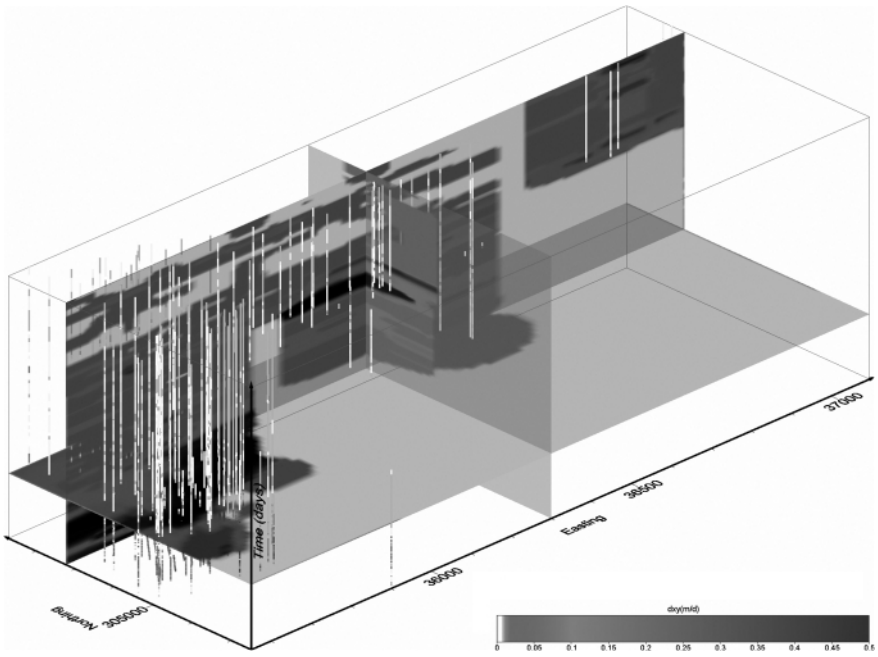

Figure 8: Space-time prism with displacement data from the Gschliefgraben landslide (y = northing (m), x = easting (m), z = time (days)). Grey level coding refers to magnitude of displacements (m/day). Lines indicate locations of monitored points over time, planes parallel to the principal axes are extracts from geostatistical space-time interpolation (xy-plane = 1 time slice). See text for details.

4. Geophysics

In the Gschliefgraben area multiple refraction and reflection seismic profiles were measured in several field campaigns lasting over five years. In all, 9.5 km of refraction seismic and 1.5 km of reflection seismic data were measured. The geophone distance differed in each field campaign, from a distance of 10 m in the early stage to 2 m for profiles measured in 2007 and 2008. Profiles with longer distances have poorer resolution but their total length is longer so features other than the actual landslide can be seen. Profiles measured in 2007 and 2008 have very short geophone spacings with high resolution, but are limited to the actual landslide. The November/December 2007 profiles were intended to obtain a clearer subsurface image of the landslide and the basement. Additionally, well logs were run in several wells, but these have steel casing so some log readings are not reliable. To correctly identify reflectors and refractors, velocity information such as sonic logs or checkshots from wells is necessary. In the Gschliefgraben, no seismic velocity information is available so the data processing and interpretation of the reflection and refraction seismic data may be wrong in terms of absolute depths.

The reflection seismic data were processed using standard processing steps (Amtmann et al., 2009). Ordinarily, it is better to interpret and model reflection seismic data in the time domain (Eichkitz at al., 2009). Because time-depth information from wells is missing, it was considered better to use stacking velocities from seismic processing to convert seismic reflection data directly into the depth domain. Therefore, all profiles are shown in depth (meters) on the vertical axis.

The focus of this work is on the suitability of seismic refraction profiles for detecting the basement of landslides. The available data were interpreted and results used to build a three–dimensional model of the subsurface in order to calculate the volume of mass moved during the last landslide and to plot arbitrary sections of the model.

Processing of seismic refraction data can be done by two methods: The classic refraction processing method (after Palmer, 1980) is based on the shortest traveltime between shot points and geophones. This results in layers that represent boundaries between geological units with different rock parameters and is suitable if there are pronounced differences in velocity between geological units and velocities increase with depth. The refraction tomography method of Schuster and Quintus-

Bosz (1993) is based on the travel time of the first arriving waves. In a first step, an initial velocity model of the subsurface is built, then velocities are changed iteratively until the computed travel times from the velocity model and the measured travel times give the best fit. It is not possible to state which refraction seismic processing method will give the best results so it is necessary to test both. For the Gschliefgraben, abrupt changes in velocities with depth are small and velocity inversion occurs, so the refraction tomography method is best. Processing results in vertical profiles in the depth domain (Fig. 5), with different color coding of the velocities in the subsurface. These profiles are loaded into Petrel (Schlumberger) seismic interpretation and modeling software as planar pictures.

Several horizons were interpreted on these refraction profiles representing changes in velocity but without layer boundaries. The identification of velocity boundaries may be uncertain because of the steady change in velocity. As there is no velocity information from wells, the bottom of the landslide cannot be clearly determined from the seismic interpretation. Nevertheless, it seems that a layer boundary with a velocity of 1700 m/s may represent the bottom of the landslide. This is supported by laserscan data and by results from other projects in comparable unconsolidated sediments. The seismic profiles are displayed together with laserscan data and the calculated difference between them is shown. On the laserscans, the surface boundary of the landslide can easily be determined. This boundary has been projected onto the refraction profiles and the most suitable velocity picked on the seismic refraction profile. In most instances, the velocity is between 1650 m/s and 1750 m/s. After the interpretation of each profile, the layers were combined and geological surfaces were generated. These surfaces are the inputs for the modeling process. Modeling of the data was also performed in Petrel, which is widely used in the oil industry to model reservoirs as arrays of regular grids. The modeling process is divided into three parts. First, the faults from the seismic interpretation are connected where necessary to build the fault model (fault modeling process). Because no faults were identified on the refraction profiles, no fault model could be built. To continue modeling, only the model boundary and the trend for the direction of the grid are defined. The second step is to generate pillars between the faults of the fault model (pillar gridding). Pillars are vertical slabs that follow the direction of the faults or trends and are the basis for the final grid. The final grid is defined by three layers, one for the top, one for the bottom and one for the middle of the model. These layers consist of rectangular cells which extend from top to bottom. In the last step, horizons are loaded into this grid, which represents a vertical layering of the grid (horizon modeling). The result is a model of five velocity layers (Fig. 6) that can be used to generate arbitrary vertical and horizontal slices and structural maps of each surface and which can be used for volume calculation.

5. Geoinformatics: Processing and analysis of monitoring data

5.1 EDA, ESDA, ESTDA

Explorative data analysis ("EDA"), explorative spatial data analysis ("ESDA") and explorative space-time data analysis ("ESTDA") are branches of (space-time) statistics that try to maximize the insight into complex data sets by uncovering the underlying trends and structures (DeSmith et al., 2009). Because of the many variables and the huge amount of monitoring results, the Gschliefgraben data were pre-processed with typical ESTDA methods, some of which are discussed below.

Plotting multiple time series graphs of displacements measured on the Gschliefgraben landslide enables to review the temporal characteristics. Fig. 7 shows time series graphs of total (xy) displacement per day for all 150 observation points (DGPS and theodolite), for the time between January, 2008 and May, 2009. There is a clear decay of displacement rates in the first four months of 2008, with displacements as low as under the dGPS detection limit in winter/spring, 2009.

Generally displacement magnitudes are biggest along the centerline of the east-west trending landslide, with a decrease towards the landslide north and south rims (see Fig. 9). In the first four months of monitoring, the decay in motions is overlaid by phases of pronounced decelerations and accelerations, which act synchronously in practically all observation points. In this time interval, correlation of motion speed and temperature (-) as well as with

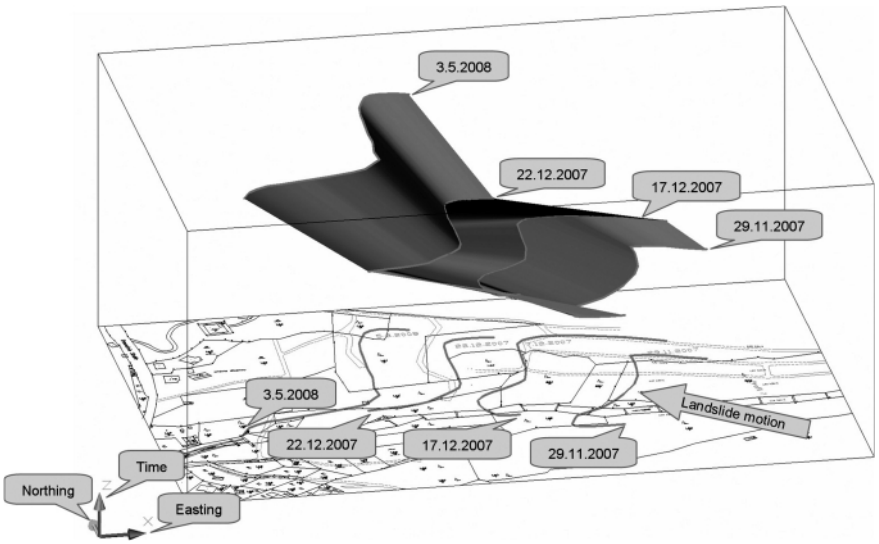

Figure 9: Development of a discontinuity zone on a map (bottom) and in the space-time prism (top). Bottom: traces of evolving shear zone, as mapped by the geologist on the Gschliefgraben landslide surface on different dates. Superimposed space-time prism: abstraction of the evolving shear zone as a surface, which acts as a boundary condition for space-time Kriging. See text for details.

precipitation (+) is possible. This is in accordance with geotechnical findings that the landslide mass was at instable balance relating to shear angles in this time interval. Originally developed in social geography, a space-time "prism" is the set of all points that can be reached by an object given a maximum possible speed from a starting point in space-time and an ending point in space-time (Miller, 1991).

In process monitoring, the space-time prism is an efficient ESTDA tool (Marschallinger, 2006): visualizing landslide surveying results in a space-time prism, stationary observation points are displayed as lines (more precisely, as series of points) which are parallel to the z axis. Observation points with constant speed show up as inclined, straight lines and accelerations / decelerations are displayed as flections in the lines. In Fig.8, color-coding these lines by displacement rate, the visualization can be enhanced (see web resource). As such, a spacetime prism is an efficient tool for visual analysis and communication of the complex space-time relationships on a landslide.

5.2 Space-time Kriging

In a space-time context, homogenization means to fill the empty volume between the observed data in the space-time prism, i.e., to interpolate them in space and time (e.g., Schafmeister, 1999). While E(ST)DA facilitates the understanding of complex processes and related hypothesis generation, for quantifying the landslide process in space and time, the observed data have to be homogenized. This is because observations are irregularly distributed in space and time due to monitoring at uneven time intervals, destruction of observation points or adding new observation points during remediation.

Geostatistical Kriging, an optimized moving average interpolator (e.g. Davis, 2002), has been used for homogenizing the displacement data. Generally, moving average interpolators are designed to portray n-dimensional, continuous variation; abrupt changes can only be handled by introducing boundary conditions. The discontinuity zones, as noticed on the Gschliefgraben landslide top surface (Riedel shears, frontal lobes) mark abrupt changes in the displacement behaviour. Mapping these zones at subsequent dates yields samples of the development of the shear zone with time. In a space-time prism, the evolution of the shear zone outcrop can be formulated as a surface that acts as a boundary condition for space-time Kriging.

Applying the boundary conditions as indicated in Fig.9, space-time Kriging yields a more detailed and realistic picture of the displacement processes associated with the Gschliefgraben landslide. In particular, abrupt changes in displacement are more reliably portrayed also in areas where only few dGPS observation points are available (Fig. 10). As such, a geologist's local knowledge is appreciated and can be incorporated into the process model.

The result of space-time Kriging the Gschliefgraben displacement monitoring data is a synthetic time series, which is portrayed as a voxel array that fills the space-time prism. Extracting voxel levels parallel to the xy plane of the space-time prism, synthetic time-slices are produced (Marschallinger, 2008). These time slices are independent of actually available monitoring data. Sequences of synthetic time slices, which are extracted at regular increments of time, are a basis for cartographic anima-

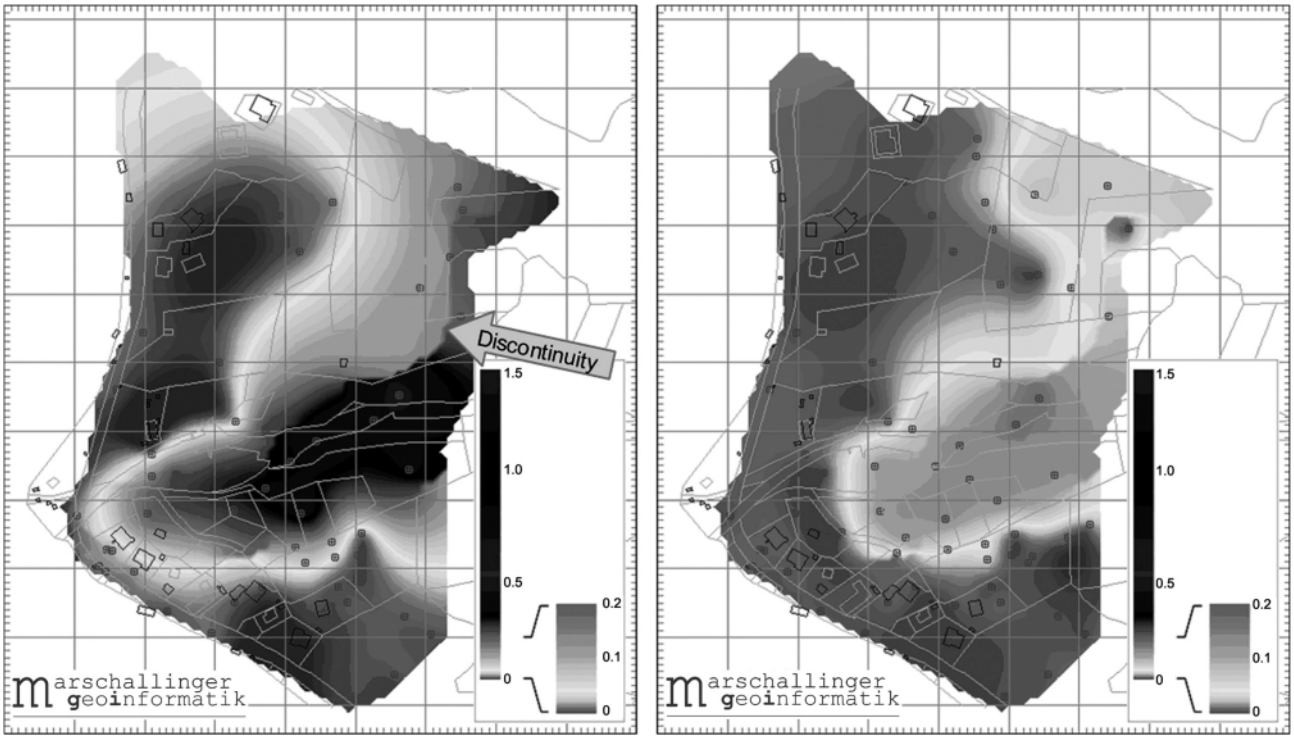

Figure 10: Synthetic time slices, as extracted from the space-time kriged displacement model of the Gschliefgraben landslide. Left: beginning of March, 2008. Right: end of March, 2008. Impact of boundary condition (Fig. 9) on interpolation is indicated by abrupt change in color (marked by arrow). Grey level coding refers to xy displacements (m/day). North = top, see text for details.

tions that portray the landslide process in its full complexness.

5.3 More ESTDA

One of the most efficient (but also costly) measures in remediating the Gschliefgraben landslide has been the extraction of subsurface water from the sliding mass. This was achieved by setting up of an array water wells (see above), most of them equipped with automatic pumps. Pumping capacity in a specific location on the landslide is directly correlated with the local subsurface water throughput. For a general documentation of pumping efficiency and as a foundation of a pumping shutdown schedule, the daily pumping quantities are displayed in a georeferenced manner as color-coded symbol maps, along with weather data to document the impact of precipitation and temperature on the water circulation in the sliding mass. As can be seen from Fig. 11 and 12, the well haulages are highly heterogeneous and spatially clustered. This is in agreement with the chaotic nature of the landslide interior (see borehole logs), where layers of pebble and sand are intercalated with a highly impermeable and plastic matrix of mudstone.

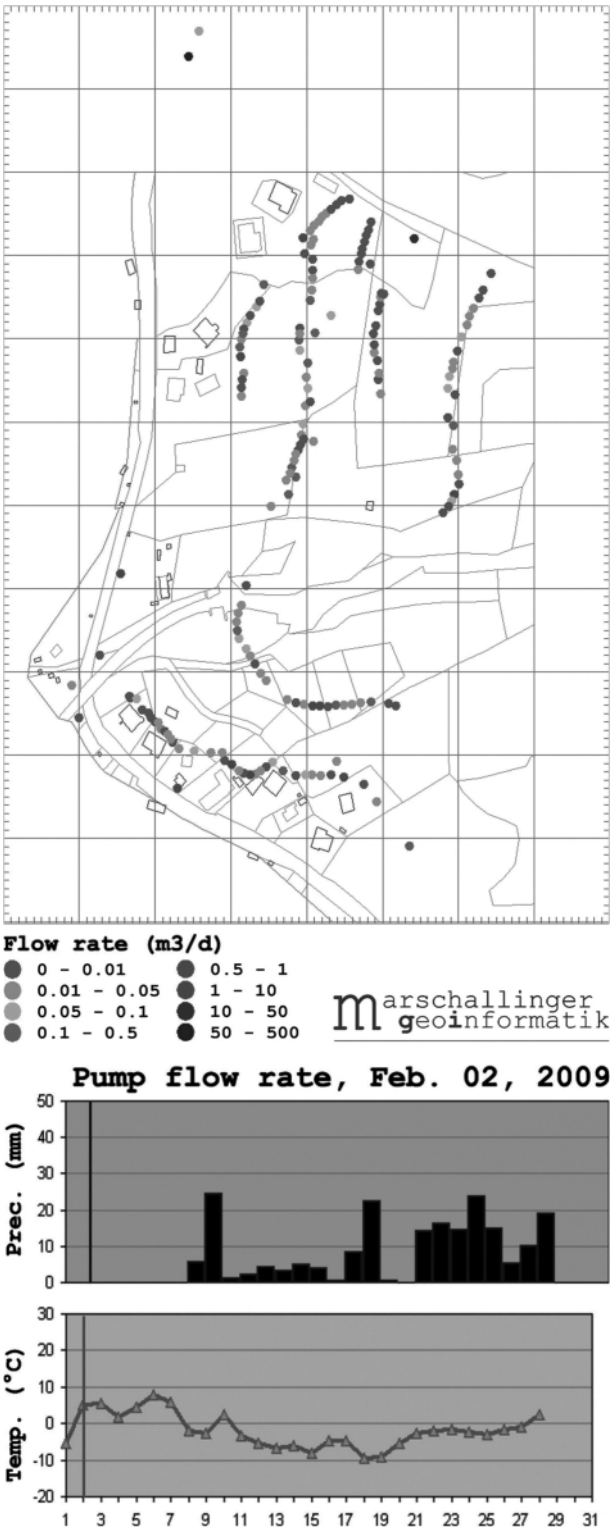

Figure 11: ESTDA graphics indicating well haulages alongside precipitation and temperature graphs February 2, 2008. Pumping quantities (in m3/day), which are indicated by grey level coded dots, have been calculated from single well haulage time series. North = top.

Quantifying haulages at random points of time necessitates interpolation to overcome the problem of unequal sampling intervals due to staff outage and individual pump breakdowns. Because of the spatially heterogeneous pumping yields, interpolation has been performed on an individual basis, providing linearly interpolated time series of single well haulages. They are the basis for the ESTDA pumping dynamics graphics (Figs. 11 and 12), provided on a daily basis. Over the total project time frame, the response of wells to precipitation is highly clustered with different response time and response intensity to rainfall. Clusters of wells with similar reaction to comparable precipitation events change their size, shape and position with time, again pointing out the highly variable and mobile substrate.

6. Soil Mechanics

6.1 The mechanics of earth and debris flows

For a description of the soil mechanics of an earth and debris flow the usual standard models are not sufficient in most cases. Formulation of forces acting on the lamellae or units of failure (according to conventional methods) or material equations (according to numerical methods) alone cannot adequately explain the fracture process. Also, extreme caution is needed in applying soil physical values obtained by laboratory studies as material behaviour is dependent upon time, stress changes, water pressure, and consistency. This non-linear material behaviour appears especially in triaxial experiments. Experiments involving varying lateral stress (vertical and horizontal pressure) and rates of loading and unloading dependent upon the position of the sample in the earth and debris flow are best suited for this purpose. A mass flow often performs an undulating downhill movement; its surface is subject to considerable, dynamic elevation and depression. The volume of moving masses may increase progressively. The use of computation methods based on soil mechanics may involve serious misinterpretation (of data) with respect to safety. In case of earth and debris flows it is often difficult or impossible to ascertain safety factors (according to the old concept of safety) or utilisation factors (according to the concept of Euro-

code 7). The same applies to estimates of failure probability. On the basis of observations, soil mechanics explorations and insights from processing (geology, soil investigation, soil property, water levels, displacement measurements) a geotechnical and soil mechanical model must be developed. According to that model the development process of the mass flow must seem plausible and possible approaches for a stabilisation must appear feasible. It is difficult to describe the complex movements and creeping processes of earth and debris flows by means of classical computation methods of soil mechanics. Furthermore, it is not easy to approach the relevant problems with the help of theories (models) of soil mechanics and geotechnology. If such theories and models are applied to locally limited areas and results of calculations misinterpreted, this may lead to wrong decisions on measures to be taken for reducing strain and relieving tension, especially regarding the sequence of such measures. Any calculation based on a soil mechanical model should be preceded by a careful observation and description of movements occurring in nature. Action and resistance are dependent upon soil weight and hydrogeological circumstances except in case of external actions such as loads or earthquakes. Movements suffer a slight dilatation in the slide or shear zone. Especially in fine-grained and low-permeability soils this change in volume leads to local pore water overpressure or internal pressure. Both phenomena have a significant influence on shear deformation behaviour.

6.2 Soil mechanical and soil physical behaviour

An earth and debris flow can have an intermittent grain structure (without supporting grain) with bound water mainly adhering to the fine fraction. If this soil mass is moved the consistency of the fine fraction (silt and clay) will change due to its high water content, passing from a soft to a liquid state relatively quickly (see figure 13). The earth and debris flow will lose its friction and turn, at least locally, into a viscous mass. The frictional component being small as a rule due to grain size, cohesion is of particular importance. In case of ingress of water and movement in the shear zone cohesion can decrease rapidly; the water released during that process can reduce normal tension in the form of pore water overpressure. In case of a sudden load of over 40 % of the possible failure stress (from observations of nature and triaxial experiments) a flowing state may ensue which may cause slope movements. “B” (figure 14) shows a system with old surfaces which are overflowed. Those surfaces are non-continuous; they are regionally bounded and consist mainly of sands and gravels with a relatively high permeability. Due to regionally limited expansion those zones are filled with water and are standing under pressure (perched groundwater table). Considered from the point of view of soil mechanics, the strained slope water conditions preceding a mass movement can be reduced by drilling wells which will provide a support for the masses flowing downhill (creeping movement, soil creeping). Water pressure (figure 15) will relieve the overlying debris flow masses and reduce friction (retentive force for the overlying debris flow). Observation of moving fronts in nature (Hofmann et al., 2008) shows that displacements are most often triggered by water through uplift, flow pressure, and softening due to grain motion. If the resisting forces of drier areas lying further down-

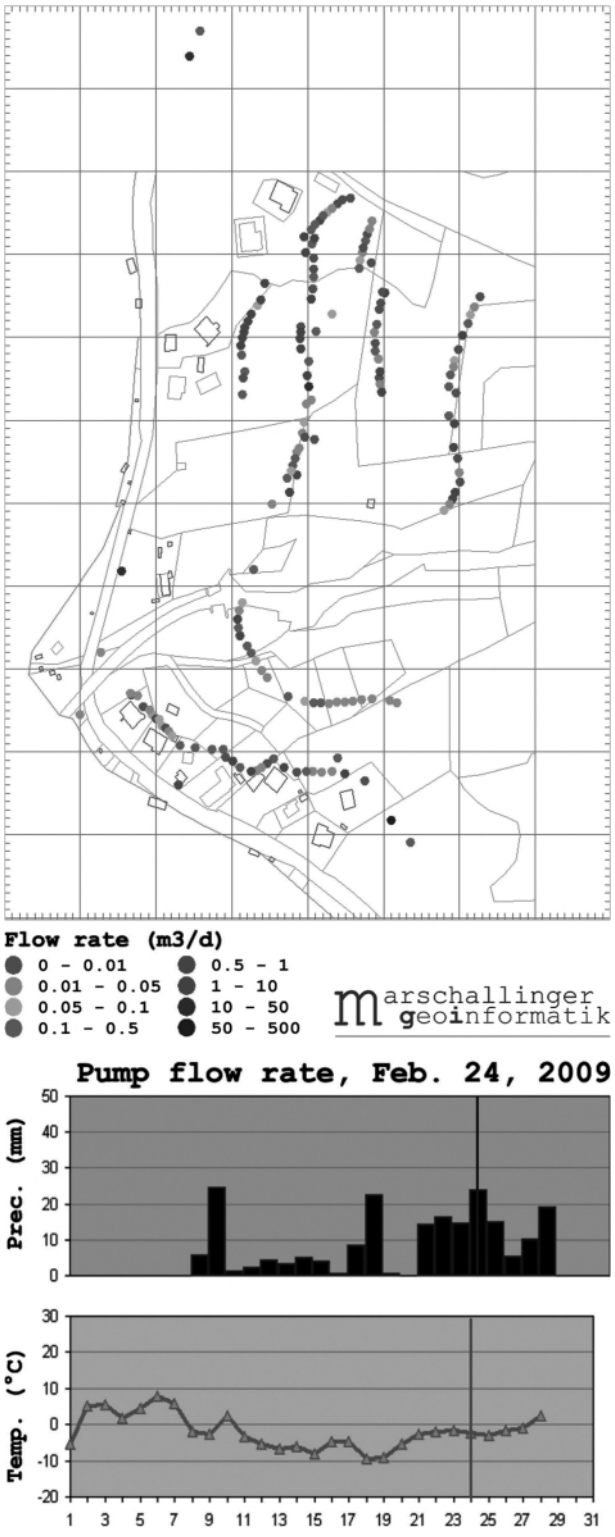

Figure 12: ESTDA graphics like Fig. 11, but time slice February 24, 2008. Only a cluster of wells to the north shows a significant reaction on the precipitations of the previous days. Compare with Fig. 11, see text for details. North = top.

hill are too strong, shear fractures will ensue, taking the form of reverse faults, with material lying farther uphill being pushed on or over the material lying farther downhill. By these movements new water passages will be opened (while old ones may be closed); additional irrigation will ensue and areas lying farther downhill will be irrigated intensively. Thus, a downhill movement will be triggered. Therefore a stabilisation of the slope is only possible before the mass movements begin; an entry of water must be prevented (figures 14 to 16).

6.3 Earth and debris flow - Soil layer A

If an earth and debris flow has an intermittent grain structure (without supporting grain) with its bound water mainly adhering to the fine fraction and if this soil mass is moved, the consistency of the fine fraction (silt and clay) will change due to its high water content, passing from a soft to a liquid state. The earth and debris flow will lose its friction and turn into a viscous mass.

6.4 Old surfaces overflowed - Soil layer B

Those surfaces are non-continuous; they are regionally bounded and consist mainly of sands and gravels with a relatively high permeability. Due to regionally limited expansion those zones are filled with water and are standing under pressure (strained slope water level). Water pressure will relieve the overlying debris flow masses and reduce friction (retentive force for the overlying debris flow).

6.5 Distinctly plastic clay – Soil layer C

These clay layers - stiff consistency - are fully saturated with water. In case of a very rapid charge (debris flow masses overflowing the soil, elevation of the area) shear strength will be reduced very quickly (pore water overpressure). This behaviour can be determined by triaxial experiments (figures 16 and 17).

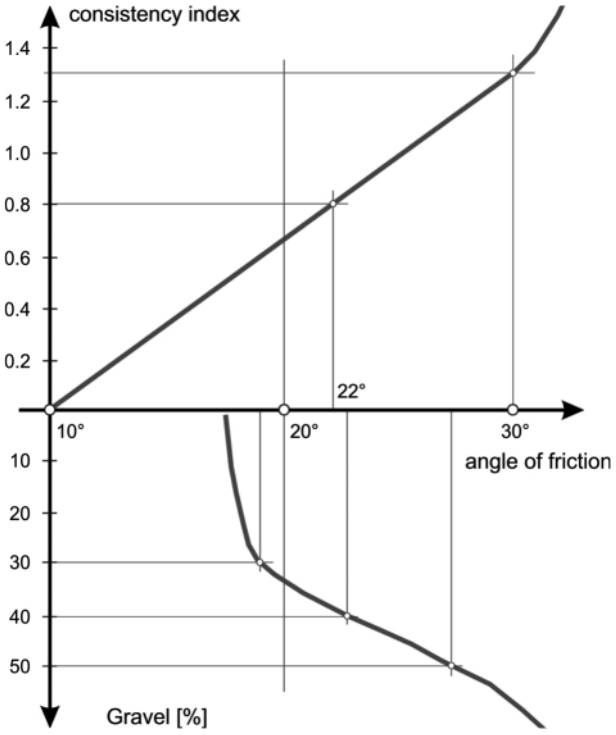

Figure 13: Dependence of the angle of friction upon consistency index. From Breymann & Hofmann (2009).

Earth and debris flows can maintain limit equilibrium for a considerable length of time (repose or creeping condition) provided that the debris flow mass (A) and the distinctly plastic clays (C) still possess sufficient shear strength (angle of friction, cohesion) for this condition of limit equilibrium. In the partly permeable sand and gravel portions of the old surfaces which are already being overflowed (B) slope water pressure under tension will develop over time as little water flows off compared to the inflow (rain, slope water). (See figure 15).

Mass movements may be triggered by various impacts, e.g. a dynamic impact combined with an increased ingress of water. At first, regional movements (elevation) of the entire layer package ensue. Those movements cause liquefaction of the debris flow masses (A), whereas in layer (B) (old surface) pressure spreads downhill ahead.

By the interaction between the spreading of water pressure in the (B) layers and the earth and debris masses flowing over them, causing elevations of several meters, an increasingly large and spreading mass movement ensues. It can be discerned as a bounded rotational movement in the front region and a subsequent translation movement of the liquefied debris flow masses (figure 15).

The kinematic behaviour of the masses discernible on the surface of an earth and debris flow can be perceived by measurement results (GPS positions, inclination and water level measurements). Every large mass movement is preceded by an increase of water pressure at the base of the moving zone (toe area). The increase of water pressure in the coarse pored areas of the “old overflowed surface” (layer B) must be distinguished from pore water overpressure in the “distinctly plastic clays” (layer C). The mass flow performs an undulating downhill movement, its surface is subject to considerable elevation and depression.

6.6 Stabilization measures

It is difficult to describe the complex movements and creeping processes of earth and debris flows by means of classical computation methods of soil mechanics. Furthermore, it is not easy to approach the relevant problems with the help of theories (models) of soil mechanics and geotechnology. If such theories and models are applied to locally limited areas and if results of calculations are misinterpreted, this may lead to wrong decisions on measures to be taken for reducing strain and tension, especially regarding the sequence of such measures. It is not economically feasible to control moving masses and ensuing forces by classical supporting measures. Such measures can even cause a deterioration of the situation. The danger of activating deeper-lying masses which may as yet be stable may outweigh the chances for those measures to succeed. Adequate stabilisation measures can be developed on the basis of the soil mechanical model; at the same time they can be adapted to the respective requirements by con-

stant comparison with in situ observations. An efficient reduction of slope water tension and adequate draining as well as the inhibition of the spread of water pressure due to a mass movement (rock slide, debris flow) are the most effective countermeasures (figure 15).

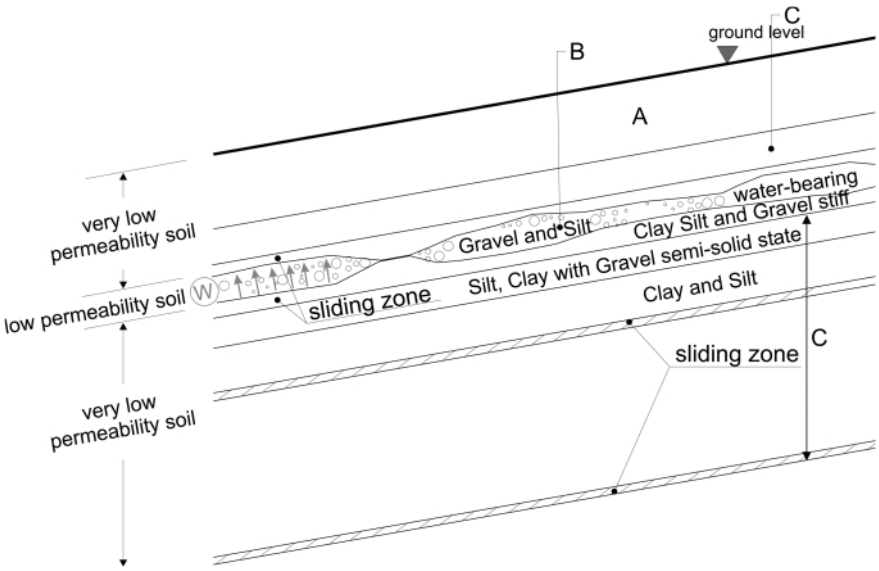

Figure 14: Diagrammatic structure of a debris flow. From Hofmann et al., (2008).

7. Mitigation measures

At the beginning of the land slide event, immediate surface water discharge measures were at the center of interest, bringing about a complete removal of vegetation at the field of activity and construction of 2.2 km of site lanes. In the course of the project, the following definitive measures were implemented (Pürstinger, 2009):

- Discharge of drained water in pipelines, which are situated outside the moving area. A total of 4.3km of pipelines was built.
- Construction of open channels for surface runoff disposal.
- Construction of longitudinal and lateral drainages for drying, ventilation and to reduce water pressure within the debris flow.
- Establishment of grooves and tongues with steel boards to retain water from entering the debris flow.
- Drilling of 281 wells with a depth of 15 - 25 m to dehydrate dehydrate and reduce water pressure in shear zones at the head of the landslide. On total, an average volume of 200 to 350m^3 water is pumped per day, with the perspective of a transition to a free surface discharge system.
- Removal of about 215000m^3 of debris from the alluvial cone to prevent lateral landslide activation
- Leveling local terrain maxima and surface sealing to reduce shear stress and to isolate subsurface water circulation from precipitation.
- Erosion control and surface consolidation by grass-seeding and afforestation.
- Setup of a permanent monitoring system for displacement observation.

8. Conclusions

The movements at the alluvial fan of the Gschliefgraben could be stopped after one and a half years of mitigation, with none of the concerned buildings damaged; as by fall 2009, mainly in the upper catchment area local displacements are observed. To implement effective countermeasures, extensive monitoring and interdisciplinary interpretation of results is mandatory: detailed geomorphological and geological field work, resulting in a large-scale map and the inclusion of subsurface exploration results was the foundation for understanding the geological and hydrological framework of the landslide. For a seamless integration of geophysical results it is essential to obtain sufficient seismic velocity information from wells with sonic logs or from checkshots. Only with this kind of data is it possible to clearly determine the 3D border between moving and nonmoving masses. Interpreting the huge amount of monitoring data acquired from active landslides calls for explorative data analysis methods for an efficient parameterization of later spatial-statistical modelling. Actuo-geological processes like landslides can be effi-

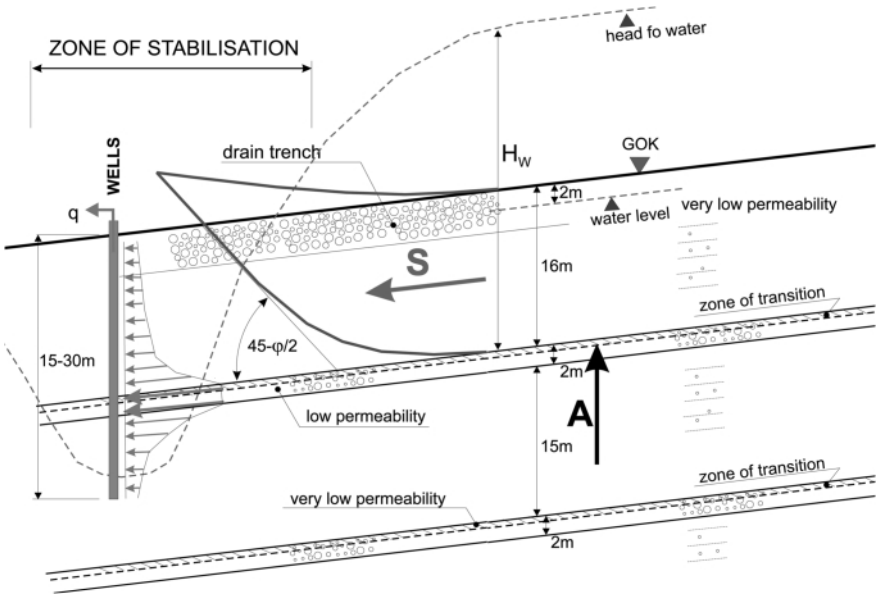

Figure 15: Mechanical behaviour of a debris flow under the influence of stabilisation measures with wells. From Hofmann et al., (2008).

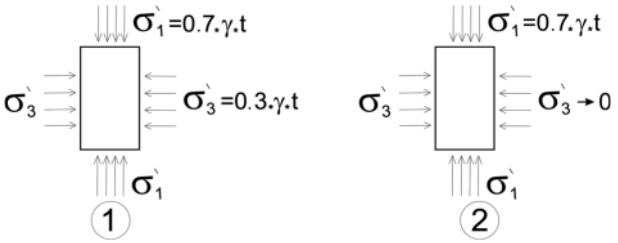

Figure 16: Conditions of tension in a triaxial experiment. From Hofmann (2008).

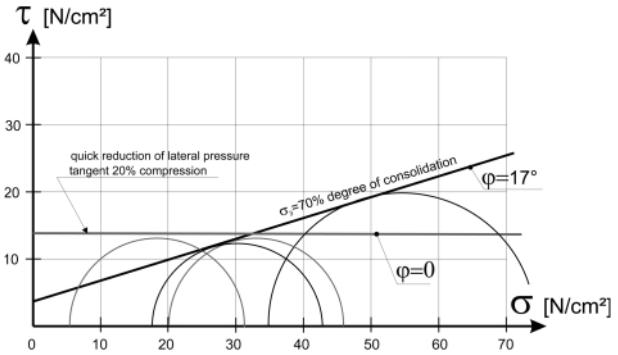

Figure 17: Time-conditioned behaviour in a triaxial experiment. From Hofmann (2008).

ciently portrayed by space-time geostatistics, providing homogeneous process models that enable quantification and seamless communication of results. For a description of the soil mechanics of an earth and debris flow the geotechnical standard models are insufficient. Formulation of forces acting on the lamellae or units of failure (according to conventional methods) or material equations (according to numerical methods) alone cannot adequately explain the fracture process. Also, extreme caution is needed in applying soil physical values obtained by laboratory studies as material behaviour is dependent upon time, stress changes, water pressure, and consistency. This non-linear material behaviour appears especially in triaxial experiments. Experiments involving varying lateral stress (vertical and horizontal pressure) and rates of loading and unloading dependent upon the position of the sample in the earth and debris flow are best suited for this purpose. To re-establish permanent settlement at the Gschliefgraben alluvial fan, in the medium term the current well pumping activities have to be replaced by a free surface discharge system; furthermore, a permanent monitoring system needs to be installed.

Acknowledgements

To a large extent, this work has been funded by the Austrian Torrent and Avalanche Control (WLV Sektion Oberösterreich). In part, this work has been funded by the Austrian Academy of Sciences. We would like to thank E. Tentschert and the anonymous reviewers for their constructive criticism.

References

Amtmann, J., Eichkitz, C.G., Schreilechner, M.G., Grassl, H. and Schmid, C., 2009. Dreidimensionale Modellierung von Massenbewegungen aus geophysikalischen Daten (Gschliefgraben, Österreich). In: Marschallinger, R., Wanker, W., Zobl, F. (Eds:). Online Datenerfassung, berührungslose Messverfahren, 3D-Modellierung und geotechnische Analyse in Geologie und Geotechnik, 254pp, Wichmann, 82-96.

Baumgartner, P., 1976. Die Massenbewegung bei Gmunden im Gschliefgraben (Traunsee, Oberösterreich) – eine Analyse aus hydrogeologischer und ingenieurgeologischer Sicht. Unpub. Doctorial Thesis, Univ. Innsbruck, 106 pp.

Baumgartner, P. and Sordian, H., 1982. Zum horizontalen und vertikalen Aufbau des Erd-Schuttströmekegels des Gschliefgrabens am Traunsee bei Gmunden (Oberösterreich). Jahrbuch Oberösterr. Museumsverein, 127/1, 227-236.

Davis, J.C., 2002. Statistics and Data Analysis in Geology. Wiley, 3rd ed., 638pp.

DeSmith, M.J., Goodchild, M.F. and Longley, P.A., 2009. Geospatial Analysis. A Comprehensive Guide to Principles, Techniques and Software Tools. Troubadour publishing, 3rd ed., 416 pp.

Egger, H. et al., 2007. Erläuterungen zu Blatt 66 Gmunden. Geologische Bundesanstalt, 66 pp.

Eichkitz, C.G, Schreilechner, M.G., Amtmann, J. and Schmid, C., 2009. Mass Movement Gschliefgraben – Interpretation and Modeling of Geophysical Data. Austrian Journal of Earth Sciences (this volume).

Gasperl, W., 2009. Massenbewegungen: Überwachung, Beobachtung und Sanierungsmöglichkeiten am Beispiel Gschliefgraben. Der Sachverständige, Heft 2/2009.

Gruber, H., Marschallinger, R., 2008. Erfassung und raum-zeitliche Interpretation von Hangbewegungen am Beispiel Gschliefgraben. Geomonitoring, FE-Modellierung, Sturzprozesse und Massenbewegungen. In: Marschallinger, R., Wanker, W. (Eds.). Geomonitoring, FE-Modellierung, Sturzprozesse und Massenbewegungen, 197pp, Wichmann, 166-182.

Jedlitschka, M., 1974. Gefahrenzonenplan der WLV. Forsttechnischer Dienst für Wildbach- und Lawinenverbauung, Gebietsbauleitung Salzkammergut.

Jedlitschka, M., 1984. Untersuchungen der Nährgebiete von Erdströmen in Hinblick auf deren Stabilisierung am Beispiel des Gschliefgrabens bei Gmunden, Oberösterreich. Proceedings Interpraevent, 2, 89-108.

Marschallinger, R., 2006. Communicating geo-relevant processes by animating the results of spatiotemporal interpolation. Proceedings IAMG 2006, Liege. IAMG 2006 CDROM.

Marschallinger, R., 2008. Geostatistical Space-Time Interpolation Used to Homogenise Hydrological Monitoring Data. Pro-

ceedings Geoinformatics Forum Salzburg, 190-198.

Miller, H. J., 1991. Modelling accessibility using space-time prism concepts within geographical information systems. International Journal of Geographical Information Systems, 5:3, 287-302.

Palmer, D., 1980. The generalized reciprocal method of seismic refraction interpretation. Society of Exploration Geophysicists, Tulsa, 104 pp.

Prey, S., 1983. Das Ultrahelvetikum-Fenster des Gschliefgrabens südöstlich von Gmunden (Oberösterreich). Jahrbuch Geologische Bundesanstalt 126-1, 95-127.

Pürstinger, C., 2009. Gschliefgraben. Projekt II 2008. Forsttechnischer Dienst für Wildbach und Lawinenverbauung, Gebietsbauleitung Salzkammergut, 46-48.

Schafmeister, M. Th., 1999. Geostatistik für die hydrogeologische Praxis. Springer, 172 pp.

Schuster, G.T. and Quintus-Bosz, A., 1993. Wavepath eikonal traveltime inversion: Theory. Geophysics 58, 1314-1323.

Singer, J. and Thuro, K., 2008. Computergestützte Auswertung von Time Domaine Reflectometry Messdaten zur Überwachung von Hangbewegungen. In: Marschallinger, R., Wanker, W. (Eds.). Geomonitoring, FE-Modellierung, Sturzprozesse und Massenbewegungen, 197pp, Wichmann, 19-34.

Weidinger, J. T. and Spitzbart, I., 2005. Beiträge zur Geologie des Gmundener Bezirks – Aus der Praxis der Geologen im Salzkammergut. Gmundener Geo-Studien, 3, 94 pp.

Weidinger, J.T., Niesner, E. and Millahn, K., 2007. Interpretation angewandt geologisch-geoelektrischer Untersuchungen in der Gschliefgraben Rutschung am Traunsee Ostufer (Gmunden/Oberösterreich). ATA Geologische Bundesanstalt, 57-72.

Received: 12. June 2009
Accepted: 22. October 2009

Robert MARSCHALLINGER[1)*], Christoph EICHKITZ[2)], Harald GRUBER[3)], Kathrin HEIBL[4)], Robert HOFMANN[5)] & Korbinian SCHMID[4)]

[1)] Austrian Academy of Sciences GIScience Research Institute, A-5020 Salzburg; Marschallinger GeoInformatik, A-5201 Seekirchen, Austria;

[2)] Inst. WasserRessourcenManagement, Joanneum Research, A-8010 Graz, Austria;

[3)] Forsttechnischer Dienst, WLV, Sektion Oberösterreich, A-4020 Linz, Austria;

[4)] Moser / Jaritz ZT-Gesellschaft f. Erdwissenschaften / Geologie, A-4810 Gmunden, Austria;

[5)] Hofmann Geotechnik, A-2380 Perchtoldsdorf, Austria;

[*)] Corresponding author, robert.marschallinger@oeaw.ac.at